

The Alaskan Arctic regime shift since 2017: A harbinger of years to come?

Thomas J. Ballinger^{a,*} and James E. Overland^b

^aInternational Arctic Research Center, University of Alaska Fairbanks, Fairbanks, AK, USA

^bNOAA/Pacific Marine Environmental Laboratory, Seattle, WA, USA

*Corresponding author; International Arctic Research Center, University of Alaska Fairbanks, 2160 Koyukuk Drive, Fairbanks, Alaska, USA 99775-7340; Email: tjballinger@alaska.edu

Revised and resubmitted to *Polar Science*

1 March 2022

Abstract

1 Recent fingerprints of Alaskan Arctic climate change include new weather patterns whose
2 impacts propagate through the Alaskan marine ecosystem. Multiple lines of observational
3 evidence draw attention to the last five years (2017-2021) as a remarkable period of change.
4 Bering Sea winter and spring ice coverage was remarkably low in 2018 and 2019 associated with
5 a shifted Aleutian Low (AL) into the western Bering Sea, and ridging of the overlying polar jet
6 stream (PJS) that supported southerly winds and reduced ice growth. The climatological
7 Beaufort High and associated Beaufort Gyre saw multiple winter-long collapses (2017 and
8 2020), the only two such events of the modern reanalysis era. In contrast, from 2012-2016 the
9 AL and PJS were located southeastward across the Gulf of Alaska, which supported sea ice
10 growth. The recent collocation of the exposed ocean surface and atmospheric anomalies supports
11 the emergence of a regional atmospheric circulation response to sea-ice loss. We propose that the
12 regional system shift after 2017 foreshadows the beginning of a period with an increasing
13 frequency of major sea-ice loss events and associated impacts – floods, delayed spring blooms,
14 and marine food chain disruptions – which is sooner than projected by climate models.

15

16 *Keywords:* Alaska, Aleutian Low, Beaufort High, Polar jet stream, Regime shift

17

18 *1. The Alaskan Arctic climate in recent years*

19 The Alaskan Arctic (**Fig. 1**) is one of the most responsive northern high-latitude regions
20 to climatic forcing. Within the past decade warming across the ocean-atmosphere interface has
21 been associated with unprecedented sea-ice change, along with enhanced interannual
22 atmospheric variability. The Beaufort High (BH) and associated Beaufort Gyre, critical features
23 in the pan-Arctic sea ice mass budget and transport, unexpectedly vanished for much of winter
24 2017 and 2020 amidst stormy weather patterns (Moore et al., 2018; Ballinger et al., 2021).
25 Meanwhile, adjacent first-year ice formation and southward advance tend to be common,
26 wintertime phenomena in the northern Bering Sea, but extreme Bering and Chukchi ice loss took
27 place in winter 2018 *and unexpectedly again* during winter of 2019 with impacts on marine
28 species and subsistence activities (Stabeno and Bell, 2019; Hauser et al., 2021). The absence of
29 cold-season sea-ice cover effectively removes the turbulent heat exchange buffer between the
30 ocean and the atmosphere and can affect synoptic processes. For example, upper-ocean heat
31 transfer aloft to the atmosphere can raise the local air pressure, and provide additional energy to
32 intermittent overlying ridges of high pressure in the polar jet stream. The amplification of these
33 waves aloft are linked to wind patterns that advect frigid Arctic air southward into the lower-
34 latitudes of downstream North America. The confluence of such surface-atmosphere interactions
35 in the Alaskan Arctic has been associated with hemispheric-scale dynamical and thermal
36 anomalies, such as the eastern North American cold winter of 2017-2018 (Tachibana et al., 2019;
37 Iida et al., 2020). Winter ice loss has also been associated with a number of important factors,
38 such as increased upward, turbulent heat exchange, decreased static stability, and increased
39 horizontal wind shear, that can intensify cyclones within the Arctic environment (Crawford et al.,
40 2022).

41 Several synthesis efforts documenting Alaskan Arctic climate change and various local
42 system-level impacts have been published in recent years (e.g., Ballinger and Rogers, 2013;
43 Wood et al. 2013; Overland et al., 2018; Danielson et al., 2020; Huntington et al., 2020). Short-
44 term atmospheric variability has been a key factor associated with such previous sub-decadal
45 warm and cold events of the historical record (Overland et al., 2012). A warm pattern emerged in
46 2014 over the ocean and adjacent terrestrial Alaska (Overland et al., 2018) with the 2014-2018
47 period marked by dramatically warmer upper ocean and lower tropospheric temperatures than
48 the respective climatological means (Thoman and Walsh, 2019; Danielson et al., 2020). This
49 recent Alaskan Arctic warming period has been connected to local atmospheric patterns and
50 processes. Danielson et al. (2020) noted strengthening of the region's ocean-ice-atmosphere
51 feedback loop and thus its memory evident in consistent physical processes since 2014. For
52 example, reduced spring sea ice has led to enhanced summer solar radiation absorption that
53 increased upper-ocean temperatures and induced elevated ocean-to-atmosphere heat fluxes and
54 amplification of autumn Pacific Arctic air temperatures with possible effects on regional cyclone
55 activity. More recently, observations suggest such an array of processes have persisted through
56 the climatological freeze period and winter season, precluding south-central Bering Sea ice
57 formation in 2018 and 2019. The unprecedented inertia of mechanisms that span the annual cycle
58 have brought about a plethora of consequences that emanate through the region's socio-
59 ecological system (Huntington et al., 2020; Hauser et al., 2021).

60 Multiple extreme events have taken place in the Alaskan Arctic during recent years
61 signaling that a regional climatic regime shift may be underway. In this paper, we turn attention
62 toward the 2017-2021 abrupt cold season changes that have occurred by evaluating atmospheric
63 observations and documenting the magnitude of these shifts relative to sub-decadal changes

64 documented in previous reports. We focus on recent winter (January – March) variability of key
65 climatological features compared with historical observations, particularly the Aleutian Low
66 (AL), BH, the pressure gradient defined by their co-variability, and the overlying polar jet stream
67 (PJS). Our goal is to offer atmospheric context and identify regional-scale climatic linkages
68 underpinning recent changes within the Alaskan Arctic system.

69 *2. A possible recent regime change in the Bering Sea*

70 An unparalleled lack of sea ice occurred in the Bering Sea during winter 2018. This event
71 cascaded to major impacts: flooding due to longer open-water fetch, delays in the spring blooms,
72 and bottom-to-top ecosystem changes from the food supply for the normally large fishery to lack
73 of sea ice habitat for walrus and ice-dependent seals (Duffy-Anderson et al., 2019; Hauser et al.,
74 2021; Mahoney et al., 2021). Winter 2018 was followed by a similar sea-ice-free event in 2019.
75 One sea-ice loss event was rare, but back-to-back events were statistically unexpected; it is
76 difficult to maintain that the second event was climatologically random.

77 For comparison to winters 2017-2021, sea-level pressure (SLP) fields averaged for
78 winters 2012-2016 (**Fig. 2a**) show the climatological atmospheric Arctic pressure gradient front
79 that supports a north–south thermal barrier north of the Bering Strait (Overland et al., 2018).
80 Associated with this pattern are strong, cold northeasterly winds that grow and advect sea ice
81 southward over the central Bering Sea. The AL center is well to the south and extends west to
82 east along the Aleutian Island chain, and the BH is well-established north of Alaska. In contrast,
83 for the recent winters (2017-2021) the AL is centered over the northwestern Bering Sea
84 supporting southerly winds over the eastern Bering Sea (**Fig. 2b**). The center of the BH is weak
85 and located further east, north of the US-Canadian border. Winters 2020 and 2021 were in fact

86 most similar to 2018 and 2019 in their position for the AL, but with a stronger north-south
87 pressure gradient north of Bering Strait.

88 Recent sea ice extents reflect southerly wind patterns (**Fig. 3**). The two lowest winters
89 (**Fig 3a**) and annual cycles of sea-ice extent occurred in 2017-2018 and 2018-2019 (**Fig. 3b**).
90 During these winters, sea-ice extent dipped 101% and 75%, respectively, below the
91 climatological mean and continued the recent period of abrupt ice loss. The dashed blue line
92 representing 2020-2021 shows that the recent year's sea ice growth slowed after January (**Fig.**
93 **3b**). The southern Bering Sea was under the influence of the AL while the northern Bering Sea
94 behaved more like a typical winter. Growth of sea ice in winter 2019-2020 also started slowly
95 and retreated in March.

96 One cause of the transition before and after 2017 is seen in the steering-level winds at
97 500 hPa (**Fig. 4**). For 2012-2016 (**Fig. 4a**), the jet stream is located well south of the Bering Sea
98 and to the east over southeastern Alaska. Geopotential height gradients are weak over the Bering
99 Sea allowing the strong climatological surface high pressure to develop. In contrast, for 2017-
100 2021 (**Fig. 4b**) the jet stream is located southward from Bering Strait. Surface low pressure in the
101 northwestern Bering Sea is supported at 500 hPa by the lobe of low geopotential heights over
102 Kamchatka. The large-scale, pan-Arctic atmospheric circulation pattern does not shift over the
103 2010-2021 period with the centers of both the tropospheric PJS (500 hPa) and the stratospheric
104 polar vortex (100 hPa, not shown) shifted off of the pole toward central Asia, with a lobe of low
105 geopotential heights toward the Sea of Okhotsk.

106 What is to be made of 2018 and subsequent events? Winter 2018 was certainly
107 unexpected, followed by its impact on the ecosystem and human populations, both local (coastal
108 communities) and distant (fisheries). Even less expected were the back-to-back 2018 and 2019

109 winter events given the large year-to-year variability of regional weather systems. Winter 2021,
110 and to a lesser extent 2020, had physical features reminiscent of winter 2018 with less sea ice
111 and a westward shifted AL. Contrasting 500 hPa height fields gives some indication of a shift
112 over the Bering Sea to a more northerly-located jet stream. Less Bering Sea ice and warmer
113 ocean temperatures could help to increase the geopotential thickness and thus disrupt the
114 orientation of the wind pattern akin to documented mechanisms of the Barents Sea region
115 (Sorokina et al., 2016). Over the record of hydrographic profiles beginning in 1966 on the Bering
116 Sea shelf, 2020 likely marked the seventh consecutive year of positive water column temperature
117 anomalies in the region (Danielson et al., 2020; Danielson, personal communication, 2021). That
118 there are no shifts in the large-scale weather pattern *beyond this region* supports the Bering Sea
119 events as having local thermodynamic causes. Given the history of winters 2017-2021, one can
120 expect a future increase in the frequency of such events and their impacts. Early winter 2021-
121 2022 shows an example of a southern location of the PJS and the earliest Chukchi sea ice
122 advance since 2012 (Thoman, personal communication, 2021); it highlights the continuing
123 importance of large-scale atmospheric interannual variability to the region.

124 *3. Unprecedented Beaufort High variability in recent years*

125 The BH pattern is a key, year-round feature in the surface pressure field of the Alaskan
126 Arctic (Ballinger and Sheridan, 2014). However, recent years have seen a decline in both BH
127 occurrence and extremes (**Fig. 5**). Winter uncharacteristically stands out in part due to BH
128 collapse in 2017 when the pressure pattern and its associated anticyclonic winds and ice motion
129 over the west Arctic were absent perhaps for the first time (in the reanalysis record) through the
130 duration of the season (Moore et al., 2018). A follow-up winter BH collapse occurred in 2020,
131 marked by the lowest March SLP (~1009 hPa) on record (Ballinger et al. 2021). Increased storm

132 activity at the expense of BH patterns in the Alaskan Arctic was a common thread across the
133 anomalous winters of 2017 and 2020. Enhanced cyclone occurrence into the region was aided by
134 the aforementioned PJS configuration and southerly wind regime across the Bering Sea.

135 Additional historical context to the BH pattern over the 2017-2021 period is provided in
136 **Fig. 5**. The two anomalous winter cases in 2017 and 2020 are defined by at least 20 fewer BH
137 days (i.e., days where $SLP > 1013$ hPa) and 10 fewer BH extremes (i.e., days where $SLP \geq 1\sigma$
138 above the 1981-2010 mean and standard deviation; **Fig. 5a,c**) than climatology. Winter 2018 saw
139 a return to above-normal occurrence of BH days (+12d) followed by a sharp reduction in 2019 (-
140 13d), and both years had below-normal occurrences of BH extremes. In 2018, the southerly
141 surface winds along the west flank of the BH supported poleward warm air advection through
142 the Bering Strait and low ice cover. In 2019, decreased BH presence coupled with the westward-
143 displaced AL promoted southerly flow that propagated storms into the Alaskan Arctic, allowing
144 low Bering ice cover to once again persist. BH hallmark collapse winters in 2017 and 2020
145 followed by anticyclone re-emergence in 2018 and 2021 collectively encompasses a sub-decadal
146 5-year period of unprecedented BH variability within the reanalysis record (**Fig. 5b,d**).

147 *4. Changes in the Beaufort and Bering Seas reflected in the regional pressure gradient*

148 A synergistic relationship exists between the AL and BH variability at weather-to-climate
149 timescale scales (Cox et al., 2019). Mechanistically, when the AL is shifted westward and the
150 BH is simultaneously centered over the Beaufort Sea, weakened, or even absent as in much of
151 winter 2017 and 2020, southerly winds supported by these configurations allow relatively warm,
152 moist flow and storm systems to propagate across the Bering Sea and into the Alaskan Arctic.
153 Conversely, if the AL is present in the western Bering Sea but the BH is shifted west over the
154 Chukchi Sea, the resulting poleward air transport through Bering Strait is blocked from entering

155 the Alaskan Arctic as in winter 2021. The covariability of these weather patterns affect processes
156 such as sea-ice melt rates and timing as well as snowmelt over terrestrial western Alaska (Cox et
157 al., 2019). In preceding sections, we showed that a change in AL position and BH occurrence
158 were both anomalous with regards to the recent string of winter seasons. The co-variability of
159 these features are further investigated by analyzing the region's winter pressure gradient across
160 the latitudinally intersecting Arctic front at three atmospheric levels: the surface (i.e., SLP), mid-
161 troposphere/PJS level (i.e., 500 hPa/z500), and lower stratosphere polar vortex level (i.e., 100
162 hPa/z100). A simple approach defines these gradients, modified from Cox et al. (2019), by
163 taking the difference of a level-specific gridpoint value within the climatological BH domain
164 (P1: 75°N, 170°W) from that in the AL domain (P2: 50°N, 170°W; as referenced in **Fig. 1**).

165 The pressure gradient analyses in **Fig. 6** support the recent regime changes with regards
166 to the AL and BH. The SLP gradient in recent years is remarkably weak reaching a 5-year
167 minima in 2017-2021 highlighted by little difference in pressure between the Beaufort and
168 Bering Seas in 2020 when the BH collapsed (**Fig. 6a**). The upper-air and surface pressure
169 gradients exhibit co-variability as z500 and z100 winter minima also occurred in 2020 with
170 record or near-record 2017-2021 means (lowest and 5th lowest 5-year means, respectively; **Fig.**
171 **6b,c**). Through time, the SLP gradient is more tightly coupled with the PJS ($r=0.92$, $p<0.05$) than
172 the lower stratosphere ($r=0.65$, $p<0.05$). Though the recent structure and intensity of the
173 stratospheric polar vortex is linked with negative (positive) surface pressure anomalies and BH
174 collapse (amplification) in 2020 and 2021, respectively (Lawrence et al., 2020; Mallett et al.,
175 2021), the long-term association points toward tropospheric dominance of the PJS on the large-
176 scale AL and BH pattern. The stronger linkage of the surface with the middle troposphere
177 relative to the stratospheric polar vortex across time suggests that the recent Alaskan Arctic

178 regime shift, characterized by anomalous atmospheric conditions in 2017-2021, is closely tied to
179 a potential ocean-atmosphere feedback between the warm ocean/thin ice, southerly atmospheric
180 circulation pattern, and associated storm activity.

181 *5. What to make of the present Alaska Arctic regime and what it may imply in the near term*

182 Studies have noted sub-decadal shifts in the Alaskan Arctic climate through the 20th and
183 into the 21st century independent of the phasing of low-frequency, large-scale climate modes
184 such as the Pacific Decadal Oscillation (Overland et al., 2012). However, the broader question
185 has been left relatively open-ended as to whether these climate shifts in regional atmospheric
186 pressure anomalies associated with AL and BH dynamics and their interactions were/are a
187 product of random internal weather variability, a limited-memory red-noise process, ongoing
188 Arctic change, or some combination. In recent years, unusual synoptic activity categorizes 2017-
189 2021 as a climatic shift relative to previous cases. As evidence, the position and magnitude of
190 atmospheric and sea ice anomalies, including westward-displaced AL patterns and low pressure
191 permeating across the Alaskan Arctic that subsumed the climatological BH and thus typical ice
192 motion in the Beaufort Gyre in 2017 and 2020, stand as unprecedented in the reanalysis record.

193 Freeze-up evaded much of south-central Bering Sea in winter 2017-18 and 2018-19, and
194 anomalous open water areas and southern ice edge positions exceeded even 2030-2044 ensemble
195 mean freeze projections from phase 5 of the Coupled Model Intercomparison Project (Wang et
196 al., 2018). These future projections of ice loss were mainly attributed to thermodynamic
197 processes with wind-driven forcing playing a secondary role. Warm ocean conditions and low
198 Bering ice coverage in 2016-17 to 2018-19 coincided with more frequent and persistent periods
199 of southerly flow (Stabeno and Bell, 2019). We suggest that continued Alaskan Arctic ice loss
200 through the winters of 2020 and 2021 was linked to the confluence of these relatively localized

201 ocean-atmosphere conditions. While not accounted for in our analyses, other factors such as a
202 diminished Bering cold pool and increased northward heat flux of Pacific water were also
203 important contributors to this recent regime shift (Danielson et al., 2020; Polyakov et al., 2020;
204 Stabeno and Bell, 2019).

205 Atmospheric extremes underscore the anomalous 2017-2021 period in the Alaskan
206 Arctic. However, as the Arctic continues to rapidly change, a related, open question is to what
207 extent that low ice coverage impacts the strength of the winds and associated atmospheric heat
208 transports into this region? Alkama et al. (2020) applied a causality approach to reanalysis data
209 (1979-2018) and found a linkage whereby winds robustly influence sea-ice loss, but the ice loss
210 also enhances Pacific Arctic winds at a lag of four months. However, recent, rapid sea-loss losses
211 may be reducing such purported lagged effects on the overlying winds. In their examination of
212 future model projections (2071-2100) from the Community Earth System Model Large
213 Ensemble, Mioduszewski et al. (2018) attributed a poleward-shifted storm track, deepened
214 winter SLP, and increased 10-m winds across the Alaskan Arctic to diminished coverage of
215 attendant local sea ice (see their Fig. 5 and 10). Observational evidence suggests that
216 atmospheric changes associated with changing Alaskan Arctic winter ice conditions that were
217 thought to be decades away may now be common features of the current climate regime. As this
218 manuscript is written, early winter 2021-22 provides another case of the regional impact of large-
219 scale PJS variability with a southward displaced North Pacific jet allowing northerly winds to
220 advect and grow sea ice more rapidly in the Chukchi and northern Bering Seas. This PJS
221 configuration, with analogous cases during years prior to 2017, underscores the key role of
222 synoptic wind patterns when local forcings (i.e., above-freezing sea surface temperatures and a
223 retreated ice edge) are not dominant. Despite the importance of large-scale winds in modulating

224 Arctic surface-atmosphere interactions, meridional PJS features tend to be underestimated in
225 climate model hindcasts, limiting the portrayal of such phenomena in the future under
226 accelerated Arctic change (Smith et al., 2020).

227 In summary, we propose that an era of new and prolonged extremes is underway in the
228 Alaskan Arctic. Accelerated open water and thin ice areas flanking the region's southern pack
229 ice boundary since 2017, thought to be decades away, is already impacting the magnitude and
230 persistence of regional weather/climate regimes, including southerly winds and storm systems.
231 Complex ocean-atmosphere interactions, largely attributed to internal variability, have been
232 linked to regional extremes through 2018 (e.g., Overland et al. 2018; Tachibana et al., 2019;
233 Danielson et al., 2020). Since then, unparalleled atmospheric, oceanic and sea-ice extremes have
234 continued to transpire, signaling a new Alaskan Arctic weather regime with an increase in the
235 interannual frequency of warm events that will be ongoing over the next decade and propagate
236 through the region's physical-ecological-human system.

237

238 *Declaration of competing interest*

239 The authors declare that they have no known competing financial interests or personal
240 relationships that could have appeared to influence the work reported in this paper.

241

242 *Acknowledgements*

243 We dedicate this paper to Dr. Kevin Wood of NOAA/PMEL, who passed away on February 14,
244 2022. The authors appreciate constructive feedback on the manuscript from Editor-in-Chief
245 Takashi Yamanouchi and two anonymous reviewers. TJB acknowledges support from ONR

246 grant N00014-21-1-2577, and JEO recognizes support from the NOAA Arctic Research

247 Program. This is PMEL contribution 5400.

248

249 **References**

- 250
- 251 Alkama, R., Koffi, E.N., Vavrus, S.J., Diehl, T., Francis, J.A., Stroeve, J., Forzieri, G., Vihma,
252 T., Cescatti, A., 2020. Wind amplifies the polar sea ice retreat. *Environ. Res. Lett.*, 15,
253 124022. doi:10.1088/1748-9326/abc379.
- 254
- 255 Ballinger, T.J., Rogers, J.C., 2013. Atmosphere and ocean impacts on recent western Arctic
256 summer sea ice melt. *Geog. Compass* 7, 686-700. doi:10.1111/gec3.12077.
- 257
- 258 Ballinger, T.J., Sheridan, S.C., 2014. Associations between circulation pattern frequencies and
259 sea ice minima in the western Arctic. *Int. J. Climatol.* 34, 1385-1394. doi:10.1002/joc.3767.
- 260
- 261 Ballinger, T.J., Walsh, J.E., Bhatt, U.S., Bieniek, P.A., Tschudi, M.A., Brettschneider, B.,
262 Eicken, H., Mahoney, A.R., Richter-Menge, J., Shapiro, L.H., 2021. Unusual west Arctic
263 storm activity during winter 2020: Another collapse of the Beaufort High? *Geophys. Res.*
264 *Lett.* 48, e2021GL092518. doi:10.1029/2021GL092518.
- 265
- 266 Cox, C.J., Stone, R.S., Douglas, D.C., Stanitski, D.M., Gallagher, M.R., 2019. The Aleutian
267 Low-Beaufort Sea Anticyclone: A climate index correlated with the timing of springtime
268 melt in the Pacific Arctic cryosphere. *Geophys. Res. Lett.* 46, 7464-7473.
269 doi:10.1029/2019GL083306.
- 270
- 271 Crawford, A.D., Lukovich, J.V., McCrystall, M.R., Stroeve, J.C., Barber, D.G., 2022. Reduced
272 sea ice enhances intensification of winter storms over the Arctic Ocean. *J. Clim.*, in press.
273 doi:10.1175/JCLI-D-21-0747.1.
- 274
- 275 Danielson, S.L., Ahkinga, O., Ashjian, C., Basyuk, E., Cooper, L.W., Eisner, L., Farley, E., Iken,
276 K.B., Grebmeier, J.M., Juranek, L., Khen, G., Jayne, S.R., Kikuchi, T., Ladd, C., Lu, K.,
277 McCabe, R.M., Moore, G.W.K., Nishino, S., Ozenna, F., Pickart, R.S., Polyakov, I.V.,
278 Stabeno, P.J., Thoman, R., Williams, W.J., Wood, K., Weingartner, T.J., 2020.
279 Manifestation and consequences of warming and altered heat fluxes over the Bering and
280 Chukchi Seas continental shelves. *Deep-Sea Res. Part II.* 177, 104781.
281 doi:10.1016/j.dsr2.2020.104781.
- 282
- 283 Duffy-Anderson, J.T., Stabeno, P., Andrews III, A.G., Cieciel, K., Deary, A., Farley, E., Fugate,
284 C., Harpold, C., Heintz, R., Kimmel, D., Kuletz, K., Lamb, J., Paquin, M., Porter, S.,
285 Rogers, L., Spear, A., Yasumiishi, E., 2019. Responses of the northern Bering Sea and
286 southeastern Bering Sea pelagic ecosystems following record-breaking low winter sea ice.
287 *Geophys. Res. Lett.* 46, 9833-9842. doi:10.1029/2019GL083396.
- 288
- 289 Fetterer, F., Knowles, K., Meier, W.N., Savoie, M., Windnagel, A.K., 2017, updated daily. Sea
290 Ice Index, Version 3.0. Boulder, Colorado USA. NSIDC: National Snow and Ice Data
291 Center. doi:10.7265/N5K072F8. [Accessed 16 February 2022].
- 292
- 293 Hauser, D.D.W., Whiting, A.V., Mahoney, A.R., Goodwin, J., Harris, C., Schaeffer, R.J.,
294 Schaeffer Sr., R., Laxague, N.J.M., Subramanian, A., Witte, C.R., Betcher, S., Lindsay,

295 J.M., Zappa, C.J., 2021. Co-production of knowledge reveals loss of indigenous hunting
 296 opportunities in the face of accelerating Arctic climate change. *Environ. Res. Lett.* 16,
 297 095003. doi:10.1088/1748-9326/ac1a36.
 298

299 Huntington, H.P., Danielson, S.L., Wiese, F.K., Baker, M., Boveng, P., Citta, J.J., DeRobertis,
 300 A., Dickson, D.M.S., Farley, E., George, J.C., Iken, K., Kimmel, D.G., Kuletz, K., Ladd, C.,
 301 Levine, R., Quakenbush, L., Stabeno, P., Stafford, K.M., Stockwell, D., Wilson, C., 2020.
 302 Evidence suggests potential transformation of the Pacific Arctic ecosystem is underway.
 303 *Nat. Clim. Change* 10, 342-349. doi:10.1038/s41558-020-0695-2.
 304

305 Iida, M., Sugimoto, S., Suga, T., 2020. Severe cold winter in North America linked to Bering Sea
 306 ice loss. *J. Clim.* 33, 8069-8085. doi:10.1175/JCLI-D-19-0994.1.
 307

308 Kalnay, E., Kanamitsu, M., Kistler, R., Collins, W., Deaven, D., Gandin, L., Iredell, M., Saha,
 309 S., White, G., Woollen, J., Zhu, Y., Chelliah, M., Ebisuzaki, W., Higgins, W., Janowiak, J.,
 310 Mo, K.C., Ropelewski, C., Wang, J., Leetmaa, A., Reynolds, R., Jenne, R., Joseph, D., 1996.
 311 The NCEP/NCAR 40-year reanalysis project. *Bull. Am. Meteorol. Soc.*, 77, 437-472.
 312 doi:10.1175/1520-0477(1996)077<0437:TNYRP>2.0.CO;2.
 313

314 Lawrence, Z.D., Perlwitz, J., Butler, A.H., Manney, G.L., Newman, P.A., Lee, S.H., and Nash,
 315 E.R., 2020. The remarkably strong Arctic stratospheric polar vortex of winter 2020: links to
 316 record-breaking Arctic Oscillation and ozone loss. *J. Geophys. Res.: Atmos.*, 125,
 317 e2020JD033271. doi:10.1029/2020JD033271.
 318

319 Mahoney, A.R., Turner, K.E., Hauser, D.D.W., Laxague, N.J.M., Lindsay, J.M., Whiting, A.V.,
 320 Witte, C.R., Goodwin, J., Harris, C., Schaeffer, R.J., Schaeffer Sr., R., Betcher, S.,
 321 Subramaniam, A., Zappa, C.J., 2021. Thin ice, deep snow, and surface flooding in Kotzebue
 322 Sound: landfast ice mass balance during two anomalously warm winters and implications
 323 for marine mammals and subsistence hunting. *J. Glaciol.* 1-15. doi:10.1017/jog.2021.49.
 324

325 Mallett, R.D.C., Stroeve, J.C., Cornish, S.B., Crawford, A.D., Lukovich, J.V., Serreze, M.C.,
 326 Barrett, A.P., Meier, W.N., Heorton, H.D.B.S., Tsamados, M. 2021. Record winter winds in
 327 2020/21 drove exceptional Arctic sea ice transport. *Commun. Earth. Environ.*, 2, 149.
 328 doi:10.1038/s43247-021-00221-8.
 329

330 Mioduszewski, J., Vavrus, S., Wang, M., 2018. Diminishing Arctic sea ice promotes stronger
 331 surface winds. *J. Clim.* 31, 8101-8119. doi:10.1175/JCLI-D-18-0109.1.
 332

333 Moore, G.W.K., Schweiger, A., Zhang, J., Steele, M., 2018. Collapse of the 2017 winter
 334 Beaufort High: A response to thinning sea ice? *Geophys. Res. Lett.* 45, 2860-2869.
 335 doi:10.1002/2017GL076446.
 336

337 Overland, J.E., Wang, M., Wood, K.R., Percival, D.B., Bond, N.A., 2012. Recent Bering Sea
 338 warm and cold events in a 95-year context. *Deep-Sea Res. Part II.* 65-70, 6-13.
 339 doi:10.1016/j.dsr2.2012.02.013.
 340

341 Overland, J.E., Wang, M., Ballinger, T.J., 2018. Recent increased warming of the Alaskan
342 Marine Arctic due to mid-latitude linkages. *Adv. Atmos. Sci.* 35, 75-84.
343 doi:10.1007/s00376-017-7026-1.
344

345 Polyakov, I.V., Alkire, M.B., Bluhm, B.A., Brown, K.A., Carmack, E.C., Chierici, M.,
346 Danielson, S.L., Ellingsen, I., Ershova, E.A., Gårdfeldt, K., Ingvaldsen, R.B., Pnyushkov,
347 A.V., Slagstad, D., Wassmann, P., 2020: Borealization of the Arctic Ocean in response to
348 anomalous advection from sub-Arctic seas. *Front. Mar. Sci.*, 7, 491.
349 doi:10.3389/fmars.2020.00491.
350

351 Smith, D.M., Scaife, A.A., Eade, R. Athanasiadas, P., Bellucci, A., Bethke, I., Bilbao, R.,
352 Borchert, L.F., Caron, L.-P., Counillon, F., Danabasoglou, G., Delworth, T., Doblas-Reyes,
353 F.J., Dunstone, N.J., Estella-Perez, V., Flavoni, S., Hermanson, L., Keenlyside, N., Kharin,
354 V., Kimoto, M., Merryfield, W.J., Mignot, J., Mochizuki, T., Modali, K., Monerie, P.A.,
355 Müller, W.A., Nicolí, D., Ortega, P., Pankatz, K., Pohlmann, H., Robson, J., Ruggieri, P.,
356 Sospedra-Alfonso, R., Swingedouw, D., Wang, Y., Wild, S., Yeager, S., Yang, X., Zhang,
357 L. *Nature*. 583, 796-800. doi:10.1038/s41586-020-2525-0.
358

359 Sorokina, S.A., Li, C., Wettstein, J.J., Kvamstø, N.G., 2016. Observed atmospheric coupling
360 between Barents Sea ice and the Warm-Arctic Cold-Siberian anomaly patterns. *J. Clim.* 29,
361 495-511. doi:10.1175/JCLI-D-15-0046.1.
362

363 Stabeno, P.J., Bell, S.W., 2019. Extreme conditions in the Bering Sea (2017-2018): Record-
364 breaking low sea-ice extent. *Geophys. Res. Lett.*, 46, 8952-8959. doi:1029/2019GL083816.
365

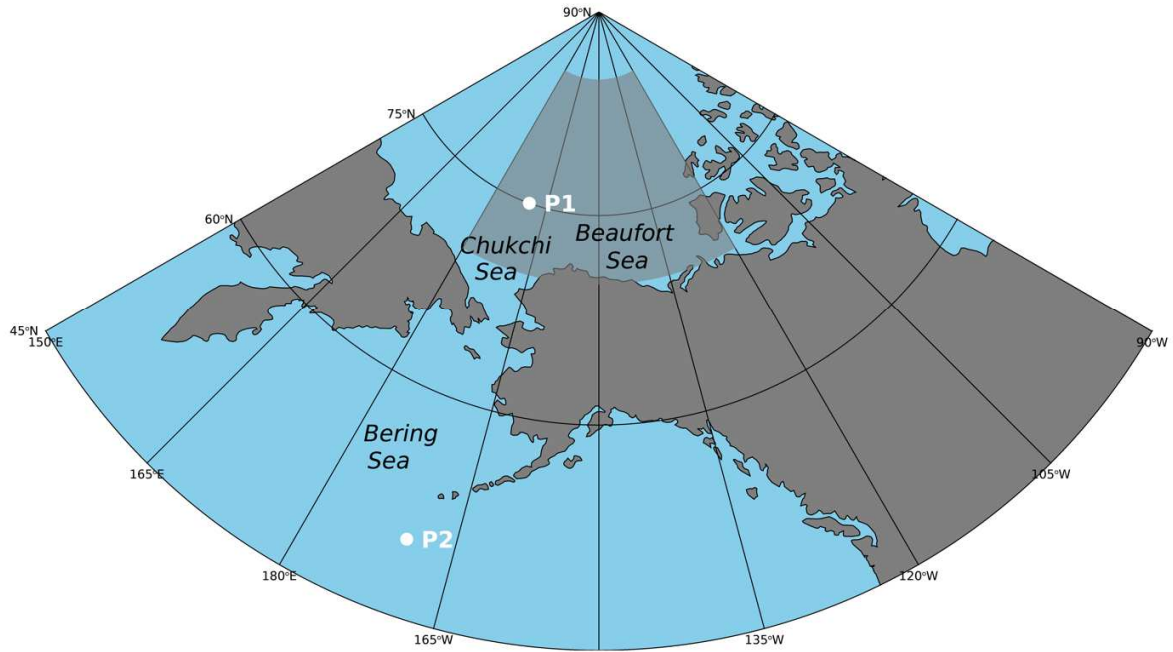
366 Tachibana, Y., Komatsu, K.K., Alexeev, V.A., Cai, L., Ando, Y., 2019. Warm hole in the Pacific
367 Arctic sea ice cover forced mid-latitude Northern Hemisphere cooling during winter 2017-
368 18. *Sci. Rep.* 9, 5567. doi:10.1038/s41598-019-41682-4.
369

370 Thoman, R., Walsh, J.E., 2019. Alaska's changing environment: documenting Alaska's physical
371 and biological changes through observations. H. R. McFarland, Ed. International Arctic
372 Research Center, University of Alaska Fairbanks.
373

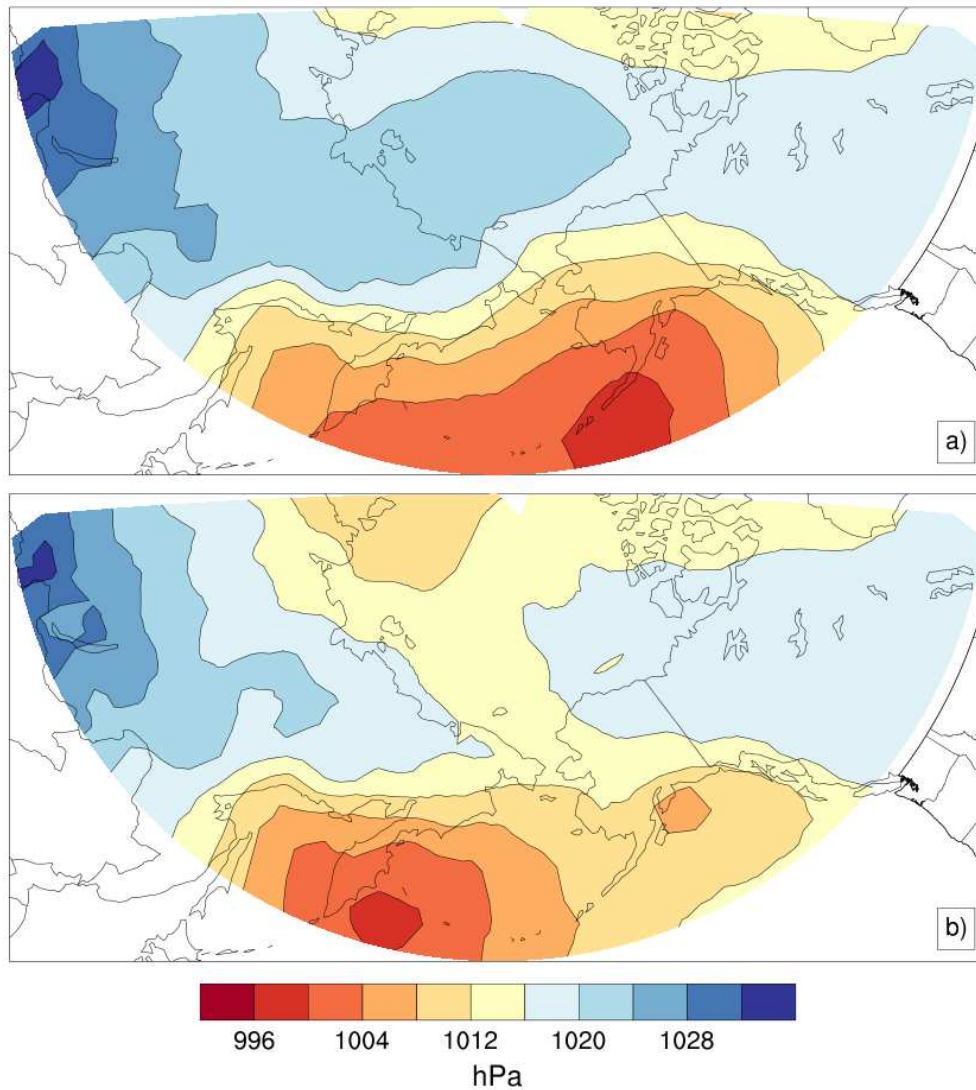
374 Wang, M., Yang, Q., Overland, J.E., Stabeno, P., 2018. Sea-ice cover timing in the Pacific
375 Arctic: The present and projections to mid-century by selected CMIP5 models. *Deep-Sea*
376 *Res. Part II.* 152, 22-34. doi:10.1016/j.dsr2.2017.11.017.
377

378 Wood, K.R., Overland, J.E., Salo, S.A., Bond, N.A., Williams, W.J., Dong, X., 2013. Is there a
379 "new normal" climate in the Beaufort Sea? *Pol. Res.* 32, 19552,
380 doi:10.3402/polar.v32i0.19552.
381

382 **Figures**

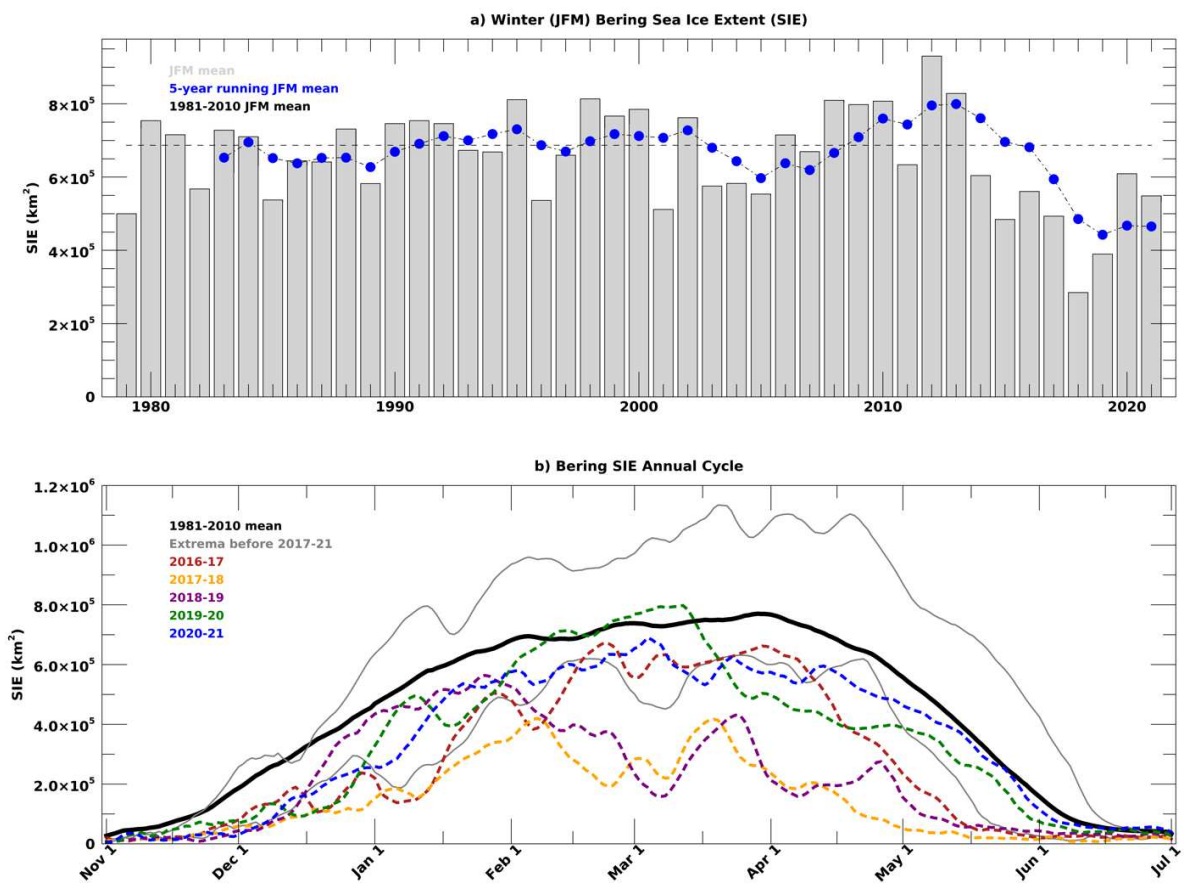


383
384 **Fig. 1.** Map centered on the Alaskan Arctic study area. The main focus regions are labeled as are
385 the Beaufort High analysis domain (light gray shaded polygon) and SLP grid points (white dots
386 labeled P1 and P2) for which analyses are presented in **Fig. 5 and 6**, respectively.
387
388

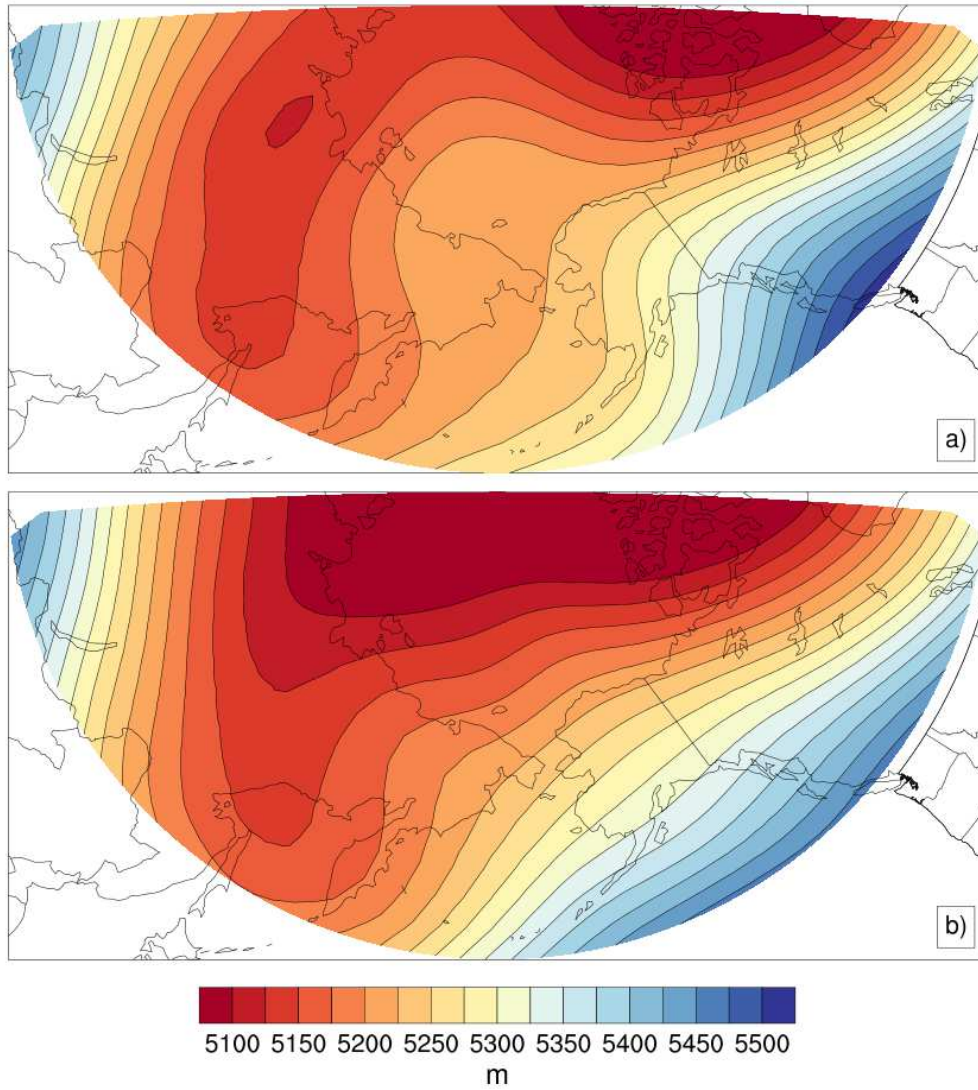


390
 391
 392
 393
 394
 395
 396

Fig. 2. Mean sea-level pressure (SLP) fields for two distinctly different atmospheric regimes. Winter (January – March; JFM) SLP is shown for 2012–2016 in a), and for 2017–2021 in b). Note the westward shift of the Aleutian Low in the more recent period. SLP data are from NCEP/NCAR reanalysis (Kalnay et al., 1996).

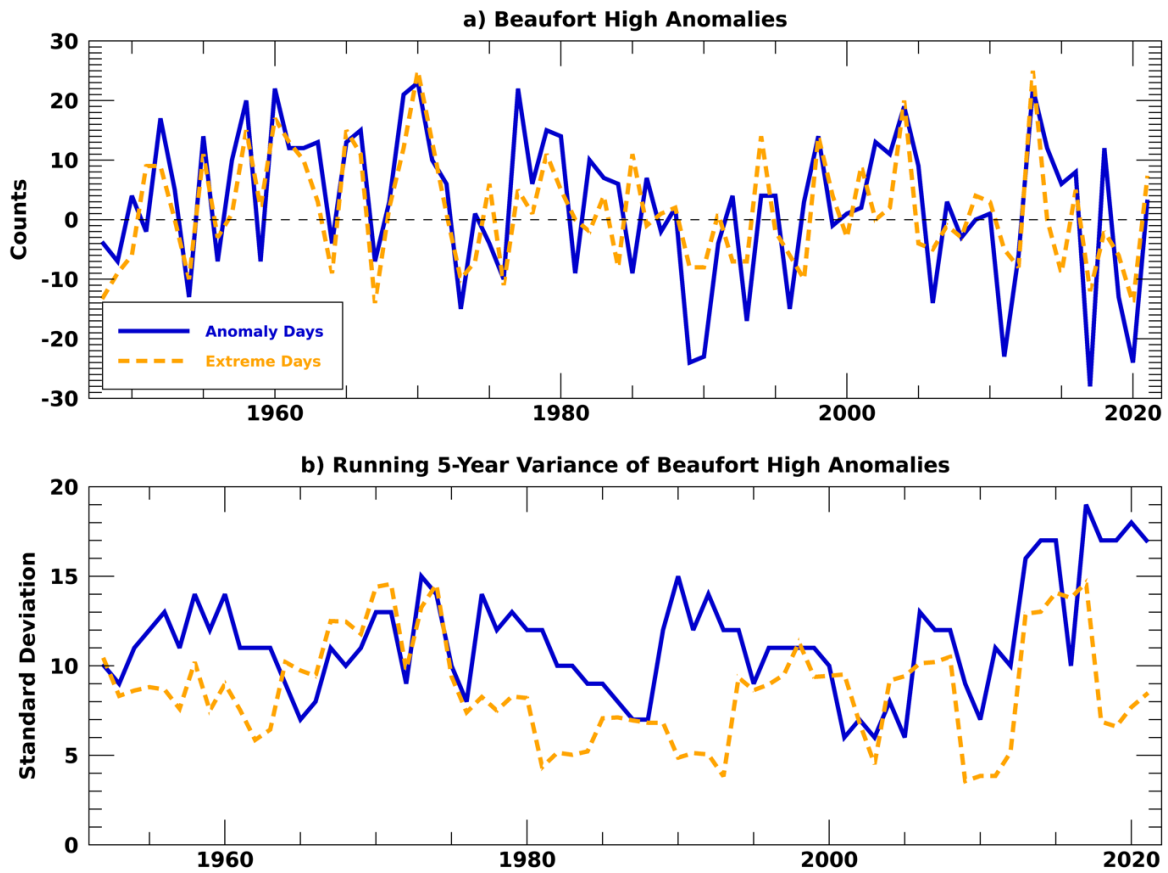
398
399

400 **Fig. 3.** Bering Sea ice extent (SIE; in km^2) from 1979-2021. In a) winter (JFM) SIE is shown
 401 with the running five-year mean and 1981-2010 climatology overlaid. The Bering SIE annual
 402 cycle is presented in b) for the 1981-2010 mean, winter extrema before 2017-21 (i.e., highest
 403 (lowest) JFM mean SIE in 2011-12 (2014-15)), and the last five annual cycles, 2016-17 to 2020-
 404 21. Data are from the Sea Ice Index obtained from the National Snow and Ice Data Center
 405 (Fetterer et al., 2017, updated daily).
 406

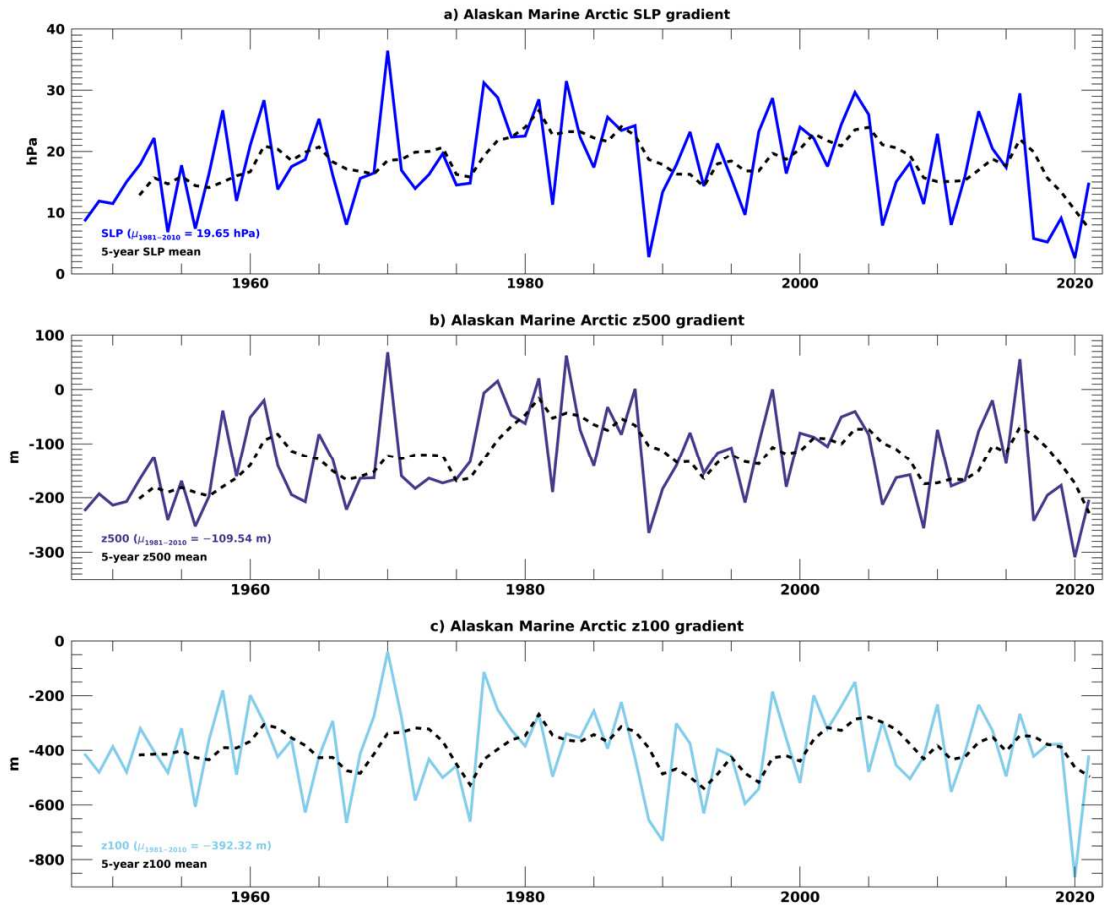


408
409
410
411
412
413
414
415

Fig. 4. Mean 500 hPa geopotential height fields (i.e., z500; in meters (m)) for the same periods isolated in **Fig. 1**. The winter (JFM) z500 field is shown from 2012-2016 in a), and for 2017-2021 in b). Geopotential height data are from NCEP/NCAR reanalysis.



417
 418 **Fig. 5.** Winter (JFM) Beaufort High Anomaly and Extreme Day counts and variability. Statistics
 419 are calculated for SLP data aggregated across the gray shaded area in **Fig. 1**. In a), counts are
 420 shown for Beaufort High (BH) Anomaly Days (blue line) and for BH Extreme Days (dashed
 421 orange line). A BH Anomaly Day is defined as such when daily SLP > 1013 hPa, while a BH
 422 Extreme Day is determined when daily SLP is $\geq 1\sigma$ from the 1981-2010 daily mean. These days
 423 are summed across the winter season, and both time series are presented with respect to the
 424 1981-2010 seasonal mean counts. In b), a running five-year standard deviation is applied to each
 425 time series in a). For example, the 1952 values represent the running variance from 1948-1952
 426 and the 2021 values are similarly calculated for the 2017-2021 period. Data are from the
 427 NCEP/NCAR reanalysis.
 428



430
 431
 432
 433
 434
 435
 436
 437
 438

Fig. 6. Winter (JFM) pressure gradients across the Alaskan Arctic. The gradients (solid lines) and corresponding 5-year running means (dashed lines) are shown across the Alaskan Arctic at three pressure levels: a) surface (i.e., SLP), b) 500 hPa (i.e., z500), and c) 100 hPa (i.e., z100). These gradients are calculated from $P1 - P2$ as shown in **Fig. 1**. Notice the pressure decrease in all three time series to record or near-record minima in the 2017-2021 era. The 1981-2010 climatological mean (μ) gradient for each level is listed in each plot for reference. Data are from the NCEP/NCAR reanalysis.